Kinematics of Roller Migration in the Planetary Roller Screw Mechanism

Matthew H. Jones
e-mail: matjones@ucdavis.edu

Steven A. Velinsky[1]
e-mail: savelinsky@ucdavis.edu

Department of Mechanical and Aerospace Engineering,
University of California, Davis,
One Shields Avenue,
Davis, CA 95616

This paper develops a kinematic model to predict the axial migration of the rollers relative to the nut in the planetary roller screw mechanism (PRSM). This axial migration is an undesirable phenomenon that can cause binding and eventually lead to the destruction of the mechanism. It is shown that this migration is due to slip at the nut–roller interface, which is caused by a pitch mismatch between the spur-ring gear and the effective nut–roller helical gear pairs. This pitch circle mismatch can be due to manufacturing errors, deformations of the mechanism due to loading, and uncertainty in the radii of contact between the components. This paper derives the angle through which slip occurs and the subsequent axial migration of the roller. It is shown that this roller migration does not affect the overall lead of the PRSM. In addition, the general orbital mechanics, in-plane slip velocity at the nut–roller interface, and the axial slip velocities at the nut–roller and the screw–roller interfaces are also derived. Finally, an example problem is developed using a range of pitch mismatch values for the given roller screw dimensions, and the axial migration and slip velocities are determined. [DOI: 10.1115/1.4006529]

Keywords: planetary roller screw mechanism (PRSM), motion analysis, kinematics, slip velocity

1 Introduction

The roller screw mechanism (RSM) [1] is a mechanical transmission device for converting rotary motion to linear motion (Fig. 1). Under some circumstances, the devices can be backdriven. Compared to the ball screw mechanism, in general, the roller screw mechanisms are capable of higher loads, longer life, higher speeds and accelerations, and finer leads (allowing for higher precision). Thus, the RSM is used in a variety of high-load, high-speed, and high-precision applications in areas such as the medical industry [2–4], aerospace industry [5,6], optical equipment [7], and robotics and high-precision machine tools [8,9].

Despite the importance and usefulness of the RSM, there has been little fundamental research to support its engineering application. Earlier work on the RSM has included research on the efficiency and failure modes [10]; dynamical load testing [11]; force, slip, and lead properties [12]; a calculation method for the elastic elements [13]; principles for evaluating wear resistance [14]; a study on the effects of wet and dry lubrications under oscillatory motion [15]; and an investigation into the static rigidity and thread load distribution [16].

There are two primary types of roller screw mechanisms—the PRSM and the recirculating roller screw mechanism. The analysis in this paper deals exclusively with the PRSM. Recently, a detailed examination of the kinematics of the PRSM has been presented by one of these authors [17]. The paper showed that though slip must occur between the rollers and the screw of the PRSM, the overall lead of the mechanism is independent of this slip. The kinematics derived in Ref. [17] assumed that there is no slip between the rollers and the nut, which is the design objective of the PRSM based on its ideal mechanical structure. However, due to manufacturing errors and/or deformations of the mechanism due to loading, the geometry of the PRSM may deviate from the ideal. In addition, for these authors no literature is known to exist on a calculation method for determining the various radii of contact, which are necessary for determining the required spur-ring gear ratio. It is a nontrivial analysis to determine these radii, as the contact may lie anywhere on the thread face, and is the subject of future research. Thus, even with perfect manufacturing, the radii of contact are likely not known with great accuracy. This uncertainty is also a likely contributor to the pitch mismatch.

Accordingly, this paper extends the kinematic model of Ref. [17] and provides a fundamental examination of the nut–roller contact slip tendency of the PRSM and the associated axial migration of the roller relative to the nut. This axial migration is an undesirable phenomenon that can cause binding and eventually lead to the destruction of the mechanism [18]. For clarity, though there are two interfaces with slip mentioned herein—at the screw–roller interface and at the nut–roller interface—this paper examines only the kinematics of slip at the nut–roller interface. First, basic properties concerning the mechanical structure of the PRSM are presented. Then the conditions that lead to slip, namely, pitch mismatch between the nut–roller and the spur-ring gear pairs, are discussed. The orbital mechanics and the angle of slip are derived, and the resulting axial migration of the roller relative to the nut is presented. It is also shown that this axial migration of the roller does not affect the pitch of the overall system. Slip velocities at the contact points are presented, and last, the needed clearance in the nut to allow for this axial migration of the roller is shown and a specific example is provided.

2 Mechanical Structure of the Planetary Roller Screw

As shown in Fig. 1, the principal elements of the PRSM are the screw shaft, nut, rollers, spur gears at both ends of each roller, and ring gears fixed at both ends of the nut. The screw and nut have a threaded profile with straight flanks and multistart threads. The rollers have a single-start thread with a rounded profile so that the contact of the components is similar to the contact between a ball and a plane. A carrier supports the rollers to ensure that they are equally spaced. While the rollers roll inside the nut, they create a

[1]Corresponding author.

Contributed by the Mechanisms and Robotics Committee of ASME for publication in the JOURNAL OF MECHANICAL DESIGN. Manuscript received July 21, 2011; final manuscript received March 22, 2012; published online April 27, 2012. Assoc. Editor: James Schmiedeler.

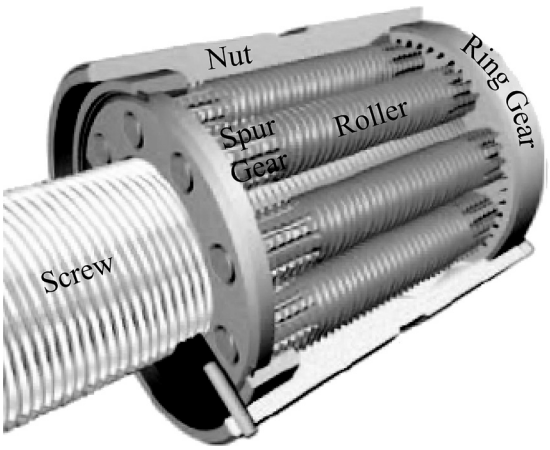

Fig. 1 Roller screw and the relevant components [20]

virtual internal thread between the screw and the nut. The virtual internal thread is exactly engaged to the threads of the screw. As was shown in Ref. [17], regardless of rolling or slipping between the screw and the roller, one revolution of the screw generates an axial displacement of the nut equal to its lead. If infinitesimally small rollers are assumed, the screw and the nut of the PRSM engage exactly like a power screw.

From the basic geometry of the typical PRSM, the leads of the screw (L_S) and the nut (L_N) are recognized to be equal, i.e., $L_S = L_N$; the helix angles of the nut (α_N) and the roller (α_R) are equal, i.e., $\alpha_N = \alpha_R$; and the components' helix radii are related as $r_N = r_S + 2r_R$, where r_N, r_S, and r_R are the radii of contact on the thread helix of the nut, screw, and roller, respectively. The relationships between the lead contact radius and helix angle of the nut and the roller, respectively, are $L_N = 2\pi r_N \tan\alpha_N$ and $L_R = 2\pi r_R \tan\alpha_R$, where L_R is the lead of the roller [17].

The primary purpose of the nut in the PRSM is to facilitate the transfer of forces from the roller screw mechanism to the external driven components [19]. For this to happen, the nut must be threaded internally so that the roller thread meshes with the nut thread. Any slip between the threads of the roller and the threads of the nut will cause the roller to slide along the helical path of its own thread and the thread of the nut. This movement will have both orbital and axial components of displacement relative to the nut. The axial component of displacement means that the roller will migrate relative to the nut and hence unscrew itself from the nut.

To attempt to eliminate any slip, the end of each roller has a spur gear that meshes with two ring gears fixed on opposite ends of the nut. The spur–ring gears are timed to match the timing of the nut–roller threaded interface, which can effectively be treated as a helical gear pair. In equation form, this is stated as [19]

$$\frac{r_N}{r_R} = \frac{G_N}{G_R} \tag{1}$$

where G_N and G_R are the spur and ring gear pitch circle radii, respectively.

With perfect component geometry and rigid body assumptions, these spur–ring gear pairs eliminate any slip and thus eliminate any axial migration of the rollers relative to the nut. This condition of no slip has been the assumption in previous kinematic studies of this mechanism [17,18]. In actual use, the nut–roller and the spur–ring gear pairs typically have a timing mismatch, represented in this paper by a pitch circle mismatch. The nut–roller and the spur–ring gears may be represented by their pitch circles, as shown in Fig. 2, with e representing the difference in the radii of the pitch circle pairs. A normalized error, ε, can also be defined as follows:

$$\varepsilon = \frac{G_N - r_N}{r_R} = \frac{G_R - r_R}{r_R} = \frac{e}{r_R} \tag{2}$$

As mentioned previously, the mismatch in the pitch circles has three possible sources: (1) manufacturing imperfections, (2) deformation of the nut–roller interface due to loading, and (3) uncertainty in the radii of contact between the components (i.e., r_R and r_N). This paper investigates the effects of this pitch mismatch on the mechanism's kinematics.

3 Orbital Mechanics With Pitch Mismatch

The operating mechanism of the components of a PRSM is analogous to the motion of a planetary gear train. While the roller is kinematically capable of slipping on the inside of the nut, the spur–ring gear pair cannot slip in the orbital plane and therefore must govern the orbital mechanics of the roller on the nut side. On the screw side, the mechanics are governed by the screw–roller effective helical radii and the friction properties at the contact surface. Though slip at the screw–roller interface does not affect the lead of the overall mechanism [17], it can be shown that any slip at the screw–roller interface will affect the axial migration of the roller relative to the nut, as the rollers will not precess around the nut.

The orbital mechanics with pitch circle mismatch can be determined according to Fig. 2. As noted above, the interaction between the threaded portions of the roller and the nut can be analogized as a helical gear pair in the orbital plane. The pitch circles are taken to be perfect for theoretical convenience such that the pitch mismatch is uniform over the circumference. Future work will focus on calculating the radii of contact, which should allow for an estimate of the pitch mismatch. The in-plane orientation of the roller can be represented by two angles: the orbital angle, θ_R, and the angle about the roller center axis, θ_r, both measured relative to a vertical axis fixed to the nut. Thus, on the nut side

$$\theta_r = \frac{G_N - G_R}{G_R}\theta_R \tag{3}$$

On the screw side, assuming no slip, the following relationship can be obtained:

$$(\theta_S - \theta_R)r_S = (\theta_r + \theta_R)r_R \tag{4}$$

where θ_S denotes the rotation angle of the screw with respect to the fixed vertical. Substitution of Eq. (3) into Eq. (4) gives

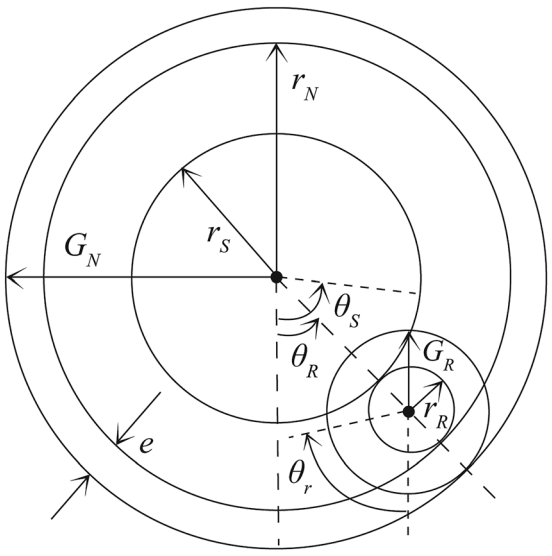

Fig. 2 Planetary gear dimensions, pitch circle mismatch exaggerated

$$\theta_R = \frac{r_S G_R}{r_S G_R + r_R G_N}\theta_S \tag{5}$$

Together, Eqs. (3) and (5) describe the orbital mechanics of the PRSM with pitch mismatch. When there is no pitch mismatch, i.e., $e = \varepsilon = 0$, and with the coordinate transformation $\theta_r = \theta'_r - \theta_R$, where θ'_r is the angle about the roller center axis measured relative to a line that extends from the center of the screw to the center of the roller (see Fig. 2), Eqs. (3) and (5) become

$$\theta_R = \frac{r_R}{r_S + 2r_R}\theta'_r \tag{6}$$

and

$$\theta_R = \frac{r_S}{2(r_S + r_R)}\theta_S \tag{7}$$

which are identical to the results provided in Ref. [17].

Both the spur gear and the threaded (helical gear) are constrained to the same body (i.e., the roller) and thus both gears must have the same angular orientation and displacement. However, to determine the angle of pure slip, the nut–roller helical gear and the spur–ring gear pairs are initially treated as separate entities. When there is a pitch mismatch, the nut–roller helical gear pair will seek to have a different orbital orientation than the spur–ring gear pair and thus the spur–ring pair will force slip to occur between the roller and the nut along their threaded interface. It is noted that the contact on the threaded interface occurs on a helical line. Thus, slip can occur on this interface as the instantaneous contact point between the roller and the screw progresses along the helix and has both orbital and axial components of motion. Essentially, the spur gear pair does not allow any slip in the orbital plane.

Figure 3 is employed to better explain the angle over which slip occurs. The nut–roller helical gear pitch circles are represented by the dashed circles and the spur–ring gear pitch circles are represented by the solid circles. The planetary motion of each component can be determined separately so that the slip angle can be determined. Each gear pair begins at the same location and same orientation. For each gear set, let the roller rotate through the same arbitrary angle, θ_r. Then, based on the kinematics of each gear pair, the spur and helical entities will end up in different final positions according to

$$\theta_R^H = \frac{r_R}{r_N - r_R}\theta_r \tag{8}$$

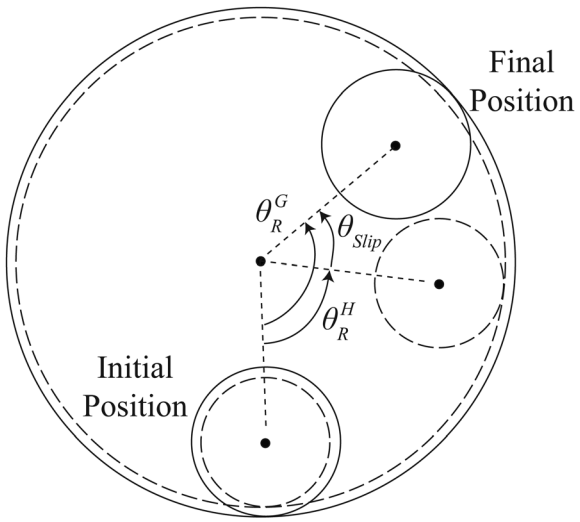

Fig. 3 Slip angle definition—Dashed lines are helical and solid lines are spur gear pairs, pitch circle mismatch exaggerated

and

$$\theta_R^G = \frac{G_R}{G_N - G_R}\theta_r \tag{9}$$

where the superscripts H and G represent the helical gear and spur gear pairs, respectively.

While the nut–roller helical pair can slip, the spur–ring gear pair cannot, and therefore must dictate the actual final orbital orientation of the roller. Thus, the nut–roller pair is forced to slip up to the position dictated by the spur–ring gear pair. Here, to better illustrate the motion, it is assumed that the motion of the helical gear (threaded portion) comprises of two components—one in which pure rolling occurs and one in which pure sliding occurs. In actuality, both occur simultaneously. The angle of pure slip between the roller and the nut is therefore

$$\theta_{\text{slip}} = \theta_R^G - \theta_R^H \tag{10}$$

With Eqs. (3), (8), and (9), and requiring that the pitch circles be concentric, the angle of slip becomes

$$\theta_{\text{slip}} = \left(1 - \frac{r_R}{G_R}\right)\theta_R \tag{11}$$

Note that Eq. (11) relates the angle of slip to the orbital orientation of the roller and makes no assumption on the slip condition between the roller and the screw. Then, with Eq. (5) and assuming no slip at the screw–roller interface, Eq. (11) becomes

$$\theta_{\text{slip}} = \left(1 - \frac{r_R}{G_R}\right)\frac{r_S G_R}{r_S G_R + r_R G_N}\theta_S \tag{12}$$

Equation (12) is the maximum slip that can occur at the nut–roller interface. Note that no slip will occur at the nut–roller interface when there is pure slip at the screw–roller interface as the rollers will not precess around the nut (i.e., $\theta_R = 0$ for all values of θ_S).

4 Axial Migration of the Roller

As noted above, any slip between the roller and the nut will occur along a helical path and will therefore have orbital and axial components of displacement. This axial component represents the axial migration of the roller relative to the nut. Since the angle of slip was determined by assuming that the spur and helical entities rotated through the same arbitrary angle θ_r in the region of pure rolling, in the region of pure slip the helical gear pair is required to slide with a fixed θ_r orientation (pure translation) according to Fig. 4. As an alternative way to visualize this, point 1 moves to point 1' with only pure slip on the nut surface, and then point 1' moves to point 1" as the roller rotates with pure slip only on the roller surface. Thus, there are two arcs of slip: the slip arc on the nut and the slip arc on the roller. The angle of slip, θ_{slip}, for both arcs is the same. These slip arcs occur along the helical path of the nut and the roller and each contributes to the axial migration of the roller.

The axial migration due to the slip arc on the nut, δ_1, can be written as

$$\delta_1 = \frac{\theta_{\text{slip}}}{2\pi}L_N \tag{13}$$

and the axial migration of the roller due to the slip arc on the roller, δ_2, is

$$\delta_2 = -\frac{\theta_{\text{slip}}}{2\pi}L_R \tag{14}$$

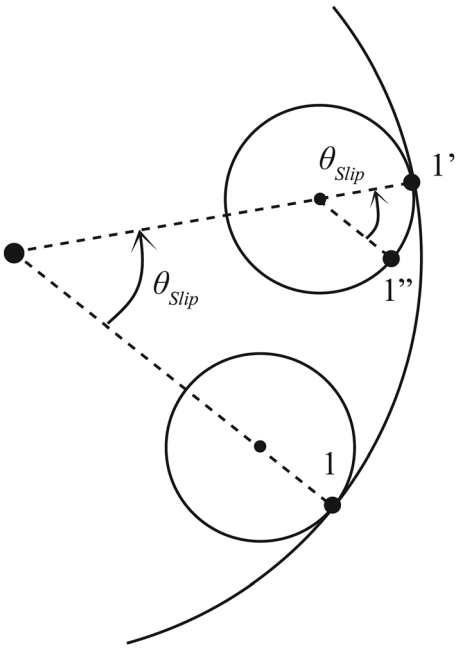

Fig. 4 Region of pure slip

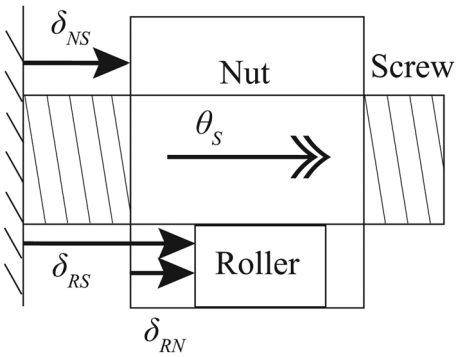

Fig. 5 Axial displacements and sign convention

where δ_1 and δ_2 are defined according to the positive displacement conventions shown in Fig. 5. Thus, the axial migration of the roller relative to the nut, δ_{RN}, is the sum of these two components, and with the relations $r_N L_R = r_R L_N$ and $L_S = L_N$ from above, becomes

$$\delta_{RN} = \left(1 - \frac{r_R}{r_N}\right)\frac{\theta_{\text{slip}}}{2\pi}L_S \tag{15}$$

With Eq. (12), the axial migration of the roller becomes

$$\delta_{RN} = \left(1 - \frac{r_R}{r_N}\right)\left(1 - \frac{r_R}{G_R}\right)\left(\frac{r_S G_R}{r_S G_R + r_R G_N}\right)\frac{\theta_S}{2\pi}L_S \tag{16}$$

Equation (16) shows that with no pitch circle mismatch, i.e., $e = \varepsilon = 0$, there is no axial migration of the roller relative to the nut, as is the design intent of the PRSM.

To prevent binding, the design of the nut of the PRSM must allow for the axial migration of the roller due to pitch mismatch. The roller axial migration over the total length of the nut's travel is given by

$$\delta_{RN}^{\text{Total}} = \left(1 - \frac{r_R G_N}{r_N G_R}\right)\frac{r_S G_R}{r_S G_R + r_R G_N}\lambda \tag{17}$$

where λ is the total length of travel of the nut. With knowledge of the axial migration, adequate dimensions and relative positioning of the mechanism's components can prevent interference and associated binding. Also, the face width of the ring gear on the nut can be made greater than the face width of the roller's spur gear to ensure adequate force transmission over the range of motion.

5 Lead of the PRSM With Pitch Mismatch

Employing the same methods as above, the displacement of the roller relative to the screw is found to be

$$\delta_{RS} = \left(\frac{r_S G_R}{r_R G_N + r_S G_R} - 1\right)\left(1 + \frac{r_S}{r_N}\right)\frac{\theta_S}{2\pi}L_S \tag{18}$$

The displacement of the nut relative to the screw, which is the lead of the PRSM, is given by

$$\delta_{NS} = \delta_{RS} - \delta_{RN} \tag{19}$$

With Eqs. (16) and (18), and after algebraic manipulation, Eq. (19) reduces to

$$\delta_{NS} = -\frac{\theta_S}{2\pi}L_S \tag{20}$$

Thus, for one revolution of the screw, i.e., $\theta_S = 2\pi$, the displacement of the nut, δ_{NS}, is equal to $-L_S$. Although the pitch circle mismatch causes the roller to migrate relative to the nut, Eq. (20) shows that the lead of the planetary screw mechanism is unaffected; i.e., regardless of whether pitch mismatch occurs or not, the mechanism's overall lead is the same.

6 Slip Velocities

Slip velocities are important for characterizing the frictional characteristics of the roller screw at the contact points. For the in-plane slip velocity at the nut–roller interface, the total arc of slip is needed. From Fig. 4, the total arc of slip, γ, is

$$\gamma = r_R\theta_{\text{slip}} + r_N\theta_{\text{slip}} \tag{21}$$

Inserting the slip angle into Eq. (21) and differentiating with respect to time leads to

$$V_P = \frac{d\gamma}{dt} = \left(1 - \frac{r_R}{G_R}\right)\frac{r_S G_R(r_R + r_N)}{r_S G_R + r_R G_N}\omega_S \tag{22}$$

where V_P is the in-plane slip velocity at the nut–roller interface and ω_S is the angular velocity of the screw. The axial slip velocity at the nut–roller interface is found by differentiating the displacement from the roller to the nut with respect to time, or

$$V_{RN} = \frac{d\delta_{RN}}{dt} = \left(1 - \frac{r_R}{r_N}\right)\left(1 - \frac{r_R}{G_R}\right)\frac{r_S G_R}{r_S G_R + r_R G_N}\frac{\omega_S}{2\pi}L_S \tag{23}$$

and the axial slip velocity at the screw–roller interface is

$$V_{RS} = \frac{d\delta_{RS}}{dt} = \left(1 + \frac{r_R}{r_N}\right)\left(\frac{r_S G_R}{r_S G_R + r_R G_N} - 1\right)\frac{\omega_S}{2\pi}L_S \tag{24}$$

The in-plane slip velocity at the screw–roller interface is beyond the scope of this paper as it involves kinetics and the friction characteristics at the screw–roller interface.

7 Dimensionless Form

Equations (3)–(24) are written in terms of the following five geometric parameters: r_R, r_N, r_S, G_R, and G_N. Based on the basic geometric relations and constraints, the equations can be normalized and put in terms of only two parameters: the normalized error in the pitch circles, ε, and the ratio of the radii of contact of the screw and roller, defined as $\phi = \frac{r_S}{r_R}$. With this substitution of variables, Eqs. (12), (16)–(18), and (22)–(24) can be rewritten in dimensionless form as

$$\theta_{\text{slip}} = \frac{\varepsilon\phi}{(\varepsilon+2)(\phi+1)}\theta_S \tag{25}$$

$$\frac{\delta_{RN}}{L_S} = \frac{\varepsilon\phi}{(\varepsilon+2)(\phi+2)}\frac{\theta_S}{2\pi} \tag{26}$$

$$\frac{\delta_{RN}^{\text{Total}}}{\lambda} = \frac{\varepsilon\phi}{(\varepsilon+2)(\phi+2)} \tag{27}$$

$$\frac{\delta_{RS}}{L_S} = -\frac{\varepsilon+\phi+2}{(\varepsilon+2)(\phi+2)}\frac{\theta_S}{\pi} \tag{28}$$

$$\upsilon_P = \frac{V_P}{r_R\omega_S} = \frac{\phi(\phi+3)\varepsilon}{(\varepsilon+2)(\phi+1)} \tag{29}$$

$$\upsilon_{NR} = \frac{V_{NR}}{L_S\omega_S} = \frac{\varepsilon\phi}{2\pi(\varepsilon+2)(\phi+2)} \tag{30}$$

$$\upsilon_{SR} = \frac{V_{SR}}{L_S\omega_S} = -\frac{\varepsilon+\phi+2}{\pi(\varepsilon+2)(\phi+2)} \tag{31}$$

These equations better illustrate the effects of the independent variables on slip, axial migration, and slip velocities of the PRSM and provide a means for better understanding the design issues.

8 Example

As an example of the developed theory, a roller screw of the following dimensions is used: $r_S = 15$ mm, $r_R = 5$ mm, and $r_N = 25$ mm. The normalized roller axial migration over the total screw length is calculated using Eq. (26) for a range of normalized pitch circle errors. The results are shown in Fig. 6. These types of plots can be used to design for axial migration, i.e., cost tradeoff between an increasing manufacturing tolerance and an increased geometric allowance for the axial migration of the roller.

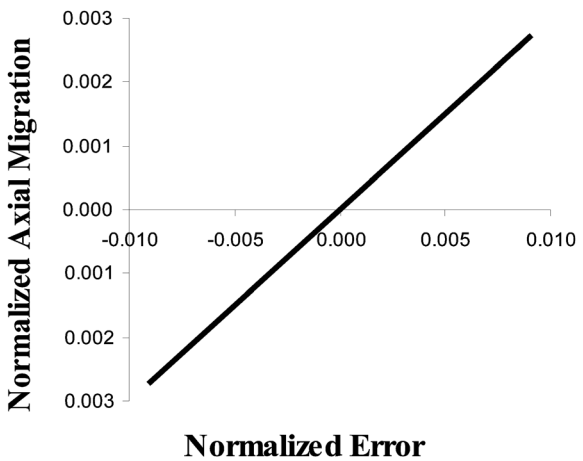

Fig. 6 Normalized total axial migration of roller, $\frac{\delta_{RN}^{\text{Total}}}{\lambda}$, as a function of pitch mismatch error, ε

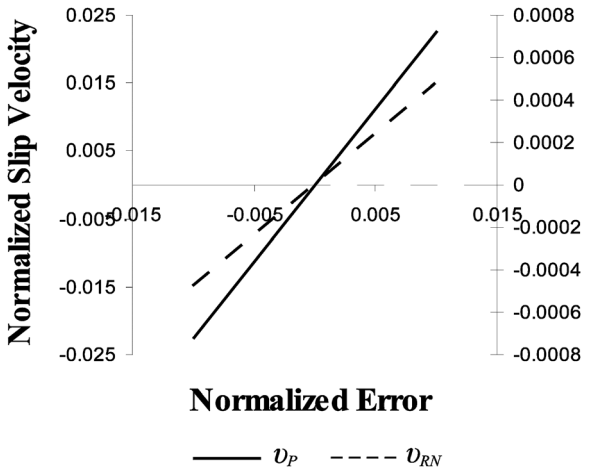

Fig. 7 Normalized slip velocity, υ_P on the left axis and υ_{RN} on the right axis as a function of pitch mismatch error, ε

The slip velocities are calculated with Eqs. (29) and (30), and the results are plotted in Fig. 7. Equation (31) was not plotted, but its results are identical to the results of Eq. (30) plus a constant of $-1/2\pi$. This constant is due to the fact that there must always be axial slip at the screw–roller interface, as shown in Ref. [17]. While the relationships shown in Figs. 6 and 7 are nonlinear, the figures show a nearly relationship over the range of values considered. As such, a linear fit over such a range could facilitate their use in design practice.

An estimate of the axial migration due to external load can be obtained based on the results from Ref. [16], which provides measured deflection of the nut assembly of a PRSM as a function of external load. This deflection is almost entirely due to deformation at the thread contacts. The corresponding deformation on the roller surface will have an axial component, approximately equal to one-fourth the deflection of the nut assembly (since there will be a corresponding deflection on the screw thread, nut thread, and opposite side of the roller), and a radial component, which will change the contact radii. Since the surface normal is approximately 45 deg from the axial direction, it can be assumed by simple geometry that the radial and axial deflections are about the same. Thus, based on the results of Ref. [16], a reasonable estimate for the change in the radius of contact due to load is about 0.0075 mm. The dimensions of the PRSM used in Ref. [16] are the same as listed above. With perfect unloaded component geometry, the corresponding normalized error is 0.0015 (Eq. (2)). With Eq. (27), the normalized axial migration is 0.00045. Thus, a total length of travel of the nut of 2000 mm corresponds to a roller axial migration equal to 0.9 mm. Note that this axial migration will occur in addition to any axial migration due to manufacturing errors, and the mechanism must account for the total axial migration to avoid binding and other detrimental behavior.

9 Conclusions

This paper analyzes the kinematics of the roller migration due to a pitch mismatch between the effective nut–roller helical gear and the spur–ring gear pairs of a planetary roller screw mechanism. The general orbital mechanics with pitch mismatch and the angle of slip at the nut–roller interface were derived. Any slip between the roller and the nut threads has been shown to cause the roller to advance along the helical contact path between the nut and the roller. In the PRSM, spur gears are affixed to the ends of each roller that mesh with ring gears at the opposite ends of the

nut. The spur gear pair ratio is intended to be the same as that of the nut–roller helical gear pair to minimize any axial advance. However, manufacturing imperfections, deformations due to load, and uncertainty in the radii of contact will cause a pitch circle mismatch between the gear pairs, which leads to axial migration of the roller. This axial migration is an undesirable phenomenon that can cause binding and eventually lead to the destruction of the mechanism.

With no slip on the screw–roller interface, the axial migration is a constant value determined by Eqs. (26) or (27), and with pure sliding at the screw–roller interface, there will be no axial migration. The true value of the axial migration will be a linear combination of the two cases. Thus, Eqs. (26) and (27) can be viewed as upper limits on the axial migration of the roller. Importantly, it was shown herein that this axial migration has no effect on the overall lead of the PRSM.

The in-plane slip velocity at the nut–roller interface as well as the axial slip velocities at the nut–roller and the screw–roller interfaces were also derived. Last, an example problem was developed using a range of pitch mismatch values for the given roller screw dimensions, and the axial migration and slip velocities were determined. Finally, the use of existing PRSM stiffness data was employed to estimate the resultant axial migration. It may be possible to deliberately design pitch mismatch into a PRSM to overcome the deformation due to forces.

Future research will consist of developing a model for the elastic deformation of the contact surfaces for use in conjunction with the results of this paper to predict the axial migration of the roller due to loading. Also, a calculation method for determining the radii of contact, which is necessary for determining the spur:ring gear ratio, is presently being developed. This information is expected to aid in the design and manufacture of PRSM.

Acknowledgment

The authors gratefully acknowledge the Division of Research and Innovation of the California Department of Transportation for the support of this work through the Advanced Highway Maintenance and Construction Technology (AHMCT) Research Center at the University of California, Davis.

References

[1] Strandgren, C. B., 1954, "Screw-Threaded Mechanism," U.S. Patent No. 2,683,379.
[2] Andrade, A., Nicolosi, D., Lucchi, J., Biscegli, J., Arruda, A. C. F., Ohashi, Y., Mueller, J., Tayama, E., Glueck, J., and Nosé, Y., 2001, "Auxiliary Total Artificial Heart: A Compact Electromechanical Artificial Heart Working Simultaneously With the Natural Heart," Artif. Organs, **23**(9), pp. 876–880.
[3] Richenbacher, W. E., Pae, W. E., Jr., Magovern, J. A., Rosenberg, G., Snyder, A. J., and Pierce, W. S., 1986, "Roller Screw Electric Motor Ventricular Assist Device," Trans. Am. Soc. Artif. Intern. Organs, **32**(1), pp. 46–48.
[4] Rosenberg, G., Snyder, A., Weiss, W., Landis, D., Geselowitz, D., and Pierce, W., 1982, "A Roller Screw Drive for Implantable Blood Pumps," Trans. Am. Soc. Artif. Intern. Organs, **28**, pp. 123–126.
[5] Gromov, V. V., Misckevich, A. V., Yudkin, E. N., Kochan, H., Coste, P., and Re, E., 1997, "The Mobile Penetrometer, A Mole for Sub-Surface Soil Investigation," *Proceedings of the 7th European Space Mechanisms and Tribology Symposium*, Noordwijk, The Netherlands, pp. 151–156.
[6] Wander, J., Byrd, V., and Parker, J., 1995, "Initial Disturbance Accommodating Control System Analysis for Prototype Electromechanical Space Shuttle Steering Actuator," *Proceedings of the American Control Conference*, Seattle, WA, Vol. 6, pp. 3961–3964.
[7] Marks, S., Cortopassi, C., DeVries, J., Hoyer, E., Leinbach, R., Minamihara, Y., Padmore, H., Pipersky, P., Plate, D., Schlueter, R., and Young, A., 1997, "The Advanced Light Source Elliptically Polarizing Undulator," *Proceedings of the Particle Accelerator Conference*, Vancouver, BC, Canada, Vol. 3, pp. 3221–3223.
[8] Brandenburg, G., Brückl, S., Dormann, J., Heinzl, J., and Schmidt, C., 2000, "Comparative Investigation of Rotary and Linear Motor Feed Drivesystems for High Precision Machine Tools," *Proceedings of the 6th International Workshop on Advanced Motion Control*, Nagoya, Japan, pp. 384–389.
[9] Dupont, P. E., 1990, "Friction Modeling in Dynamic Robot Simulation," *Proceedings of the IEEE International Conference on Robotics and Automation*, Cincinnati, OH, Vol. 2, pp. 1370–1376.
[10] Lemor, P. C., 1996, "The Roller Screw, An Efficient and Reliable Mechanical Component of Electro-Mechanical Actuators," *Proceedings of the 31st Intersociety Energy Conversion Engineering Conference, IECEC*, Washington, DC, Aug. 11–16, Vol. 1, pp. 215–220.
[11] Schinstock, D. E., and Haskew, T. A., 1996, "Dynamic Load Testing of Roller Screw EMAs," *Proceedings of the 31st Intersociety Energy Conversion Engineering Conference*, *IECEC*, Washington, DC, Aug. 11–16, Vol. 1, pp. 221–226.
[12] Hojjat, Y., and Agheli, M. M., 2009, "A Comprehensive Study on Capabilities and Limitations of Roller–Screw With Emphasis on Slip Tendency," Mech. Mach. Theory, **44**(10), pp. 1887–1899.
[13] Tselishchev, A. S., and Zharov, I. S., 2008, "Elastic Elements in Roller-Screw Mechanisms," Russ. Eng. Res., **28**(11), pp. 1040–1043.
[14] Sokolov, P. A., Blinov, D. S., Ryakhovskii, O. A., Ochkasov, E. E., and Drobizheva, A. Y., 2008, "Promising Rotation-Translation Converters," Russ. Eng. Res., **28**(10), pp. 949–956.
[15] Falkner, M., Nitschko, T., Supper, L., Traxler, G., Zemann, J. V., and Roberts, E. W., 2003, "Roller Screw Lifetime Under Oscillatory Motion: From Dry to Liquid Lubrication," *Proceedings of the 10th European Space Mechanisms and Tribology Symposium*, pp. 297–301.
[16] Jiajun, Y., Zhenxing, W., Jisheng, Z., and Wei, D., 2011, "Calculation of Load Distribution of Planetary Roller Screw and Static Rigidity," J. Huazhong Univ. Sci. Technol. (Natural Science Edition), **39**(4), pp. 1–4.
[17] Velinsky, S. A., Lasky, T. A., and Chu, B., 2009, "Kinematics and Efficiency Analysis of the Planetary Roller Screw Mechanism," ASME J. Mech. Des., **131**, p. 011016.
[18] Sokolov, P. A., Ryakhovskii, O. A., Blinov, D. S., and Laptev, A., 2005, "Kinematics of Planetary Roller–Screw Mechanisms," Vestn. MGTU, Mashinostr., **2005**(1), pp. 3–14.
[19] Ryakhovskii, O. A., Blinov, D. S., and Sokolov, P. A., 2002, "Analysis of the Operation of a Planetary Roller–Screw Mechanism," Vestn. MGTU, Mashinostr., **2002**(4), pp. 52–57.
[20] SKF, "Roller Screws," *SKF Group*, accessed January 5, 2011, http://www.skf.com/files/779280.pdf